Vol. 46 (2015) ACTA PHYSICA POLONICA B No 8

THE ECCENTRIC COLLECTIVE BFKL POMERON*

Larry McLerran

RIKEN BNL, Brookhaven National Laboratory, Upton, NY 11973, USA
and
Physics Department, Brookhaven National Laboratory, Upton, NY 11973, USA
and
Physics Department, China Central Normal University, Wuhan, China

Vladimir V. Skokov

Department of Physics, Western Michigan University, Kalamazoo, MI 49008, USA
vladimir.skokov@wmich.edu

(Received May 4, 2015)

We apply the flow analysis for multi-particle correlations used in heavy-ion collisions to multi-particle production from a Pomeron. We show that the n^{th} order angular harmonic arising from an m particle correlation $v_n[m]$ satisfies $v_n[m] \approx v_n[p]$ for $n \geq 1$. We discuss some implications of this for the Color Glass Condensate description of high energy hadronic collisions.

DOI:10.5506/APhysPolB.46.1513
PACS numbers: 12.38.Mh, 12.38.Aw

1. Introduction

The BFKL pomeron is presumably responsible for driving the high energy growth of cross sections in high energy hadronic collisions [1]. In parton–parton scattering, the Pomeron would correspond to the ladder graph diagram of Fig. 1. In Fig. 1, we will consider the imaginary part of this diagram corresponding to multi-gluon production. For such a process, the momentum of the particles initiating the Pomeron exchange at the top and the bottom of the diagram are equal in the initial and final state, so that the momentum on the struts of the ladder are equal. If the momentum transfer imparted to the struts, q, is large, this diagram can be evaluated in weak coupling and gives the perturbative BFKL pomeron. The BFKL pomeron leads to evolution of quark and gluons distribution functions through the BFKL equation [1].

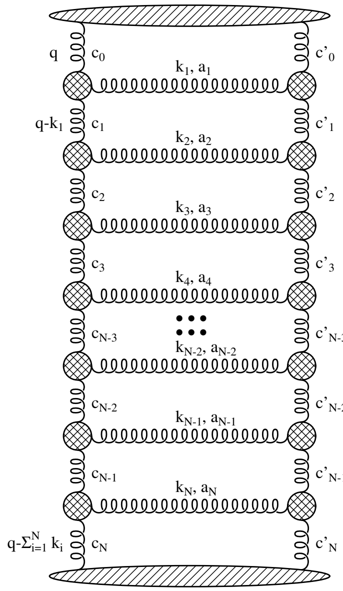

Fig. 1. N-gluon production. The shaded blob denotes Lipatov vertex.

In theories of gluon saturation [2–5], the momentum scale associated with Pomeron exchange is that of the saturation momenta, and the evolution equation for the saturation momentum is basically derivative of that of evolution of the BFKL pomeron. The basic content of the Color Glass Condensate description of such processes is that the sources at the top and bottom of the ladder are replaced by a distribution of colored sources. These color sources are coherent, so that the infrared integrations over momentum transfer are cut-off at the saturation momenta of the upper and the lower hadron participating in the collision. When computing multi-particle production, one is determining inclusive particle production with such a diagram, and one should look only over a finite range of rapidity between the upper produced gluon and the lower produced gluon. The saturation momentum of the upper hadron is at that of the upper rapidity and similarly for the lower hadron. The restriction on the total rapidity is that it is of the order of $\alpha_{\rm s} N_c \Delta y \ll 1$. As we will show by explicit computation, the rapidity distribution of the produced particles is flat in this case.

When one considers multi-gluon correlations, there are a variety of possible effects. In this paper, we will compute the contribution arising from the Pomeron. In general, in hadron collisions, there are contributions from final state interactions. In heavy-ion collisions, AA [6, 7] and also perhaps high multiplicity pp [8] and pA [9] these may be the dominant effects [10]. In addition, there are two-particle correlations generated by the initial state of such collisions. In particular, there is the two-particle correlation generated in the CGC. The diagram of Fig. 2 generates such a correlation [11–13]. It is of leading order in the classical approximation but suppressed by $1/N_c^2$ in the large number of colors limit.

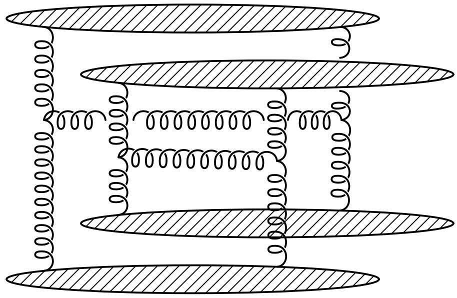

Fig. 2. The Glasma graph.

The diagrams we consider arising from Pomeron exchange are of higher order in α_s than are the two-particle correlation diagrams usually considered for the Color Glass Condensate. They are however a factor of N_c^2 larger. Note also that in the case of pp or pA collisions, the Pomeron diagram is also enhanced due to density factors associated with the coupling of the correlated diagram to the CGC. For example, if one couples to a dilute projectile with a classical field strength of the order of g, and a dense particle target with strength $1/g$, we have the following cases for two-gluon production:

System	Pomeron graph	Glasma graph
Dense–Dense	1	$1/g^4$
Dilute–Dense	g^4	g^4
Dilute–Dilute	g^8	g^{12}

Such counting is, of course, simplistic, since if we are at small enough momenta, we are in the region where the saturation momenta of the proton is important, and then the counting of powers of g in proton–proton collisions is similar to that of heavy ions. Another subtlety for heavy-ion collisions or high multiplicity events is that the overall normalization of the flow contributions is scaled by the production cross section with no angular dependence, and this contains contributions from multiple particle processes that involve many gluon exchanges, and are in addition to the contribution of the Pomeron. To properly compute the factors associated with the typical Glasma diagram and that of the Pomeron is, of course, not so easy to do, but our point is that we might expect the Pomeron to play an increasingly important role in pp and pA collisions relative to AA.

In any case, how one resolves the Pomeron and separates it from other effects is not the goal of this paper. Our much more modest goal is to explore the multi-particle correlations associated with the Pomeron decay into gluons. We find that there is a rich structure of correlations, and in particular, we find that the multi-particle moments satisfy $v_n[p] \approx v_n[m]$. This approximate equality is a signature of the collectivity of motion of the gluons produced from a single Pomeron. Its origin is not hydrodynamical but is associated with the collectivity of the underlying emission process. It might be possible to isolate and study such processes in electron–positron annihilation experiments and in deep inelastic scattering experiments. These correlations are induced by the transverse momentum conservation; however, the collectivity comes in as a uniform distribution in rapidity originating from the BFKL ladder. Another important aspect of the BFKL treatment is that the transverse momentum conservation alone does not guarantee the approximate equality $v_n[m] \approx v_n[p]$.

2. Angular correlations in gluon bremsstrahlung

We first analyze the two-particle correlation induced in a single Pomeron decay. Our analysis parallels the insightful work of Gyulassy, Levai, Vitev and Biro [14] of the underlying process of gluon bremsstrahlung first analyzed by Bertsch and Gunion [15].

The formula for multiple gluon production using the Lipatov vertex formalism valid in large N_c for high energy multi-gluon production is

$$\frac{d^{3N}\sigma}{dy_1 d^2k_1 dy_2 d^2k_2 \ldots dy_N d^2k_N} = f \int d^2q_\perp \frac{1}{q_\perp^2 + \mu^2} \frac{1}{\left(\vec{q}_\perp - \sum_{j=1}^{n} \vec{k}_{\perp j}\right)^2 + \mu^2} \prod_{i=1}^{N} \frac{1}{k_{\perp i}^2} \,. \tag{1}$$

The overall factor f depends on the particular system, for dilute–dilute scattering $f = \frac{1}{2}(4g^2)^{N+2} C_A^N C_F N_c$, where $C_A = N_c$ and $C_F = \frac{N_c^2-1}{2N_c}$.

In this formula, N particles are produced with transverse momenta k_i and rapidity y_i. The factors of μ^2 in this cross section are infrared cutoff squared, which in the saturation picture, is the saturation momentum, Q_s. In Eq. (1), we neglect virtual corrections which reggeize the gluons in the struts of the ladder, because our main goal is to compute gluon production in the rapidity region with the width much less than $1/\alpha_\mathrm{s}$, where α_s should be computed at the momentum scale of the interest — the saturation momentum, Q_s. This approximation was also used in Ref. [16] to compute the two-particle correlation function. Also, in general, Eq. (1)

involves unintegrated gluon distribution functions associated with the target and projectile. To simplify computations, we approximate the distribution functions by trivial ones.

A useful relation that later will be applied in our analysis is

$$1 = \int d^2p_\perp \delta\left(\vec{p}_\perp + \vec{q}_\perp - \sum_i \vec{k}_{\perp i}\right) = \int \frac{d^2p_\perp}{(2\pi)^2} \int d^2x_\perp e^{i\vec{x}_\perp\left(\vec{p}_\perp + \vec{q}_\perp - \sum_i \vec{k}_{\perp i}\right)} . \tag{2}$$

Use of this relation allows integration over the final-state momenta in a way that exploits the fundamental factorization of the integrated N particle production amplitude.

3. Two-particle production

Let us begin by computing v_n for the two-particle amplitude. We first write down a formula for the integrated two-particle correlation projected onto an angular dependence $e^{in\phi}$

$$\begin{aligned}
\frac{d^2\sigma_n}{dy_1 dy_2} &= f\int \frac{d^2k_{1\perp}}{k_{1\perp}^2} e^{i\phi_1 n} \int \frac{d^2k_{2\perp}}{k_{2\perp}^2} e^{-i\phi_2 n} \int \frac{d^2q_\perp}{q_\perp^2+\mu^2} \frac{1}{\left(\vec{q}_\perp - \vec{k}_{1\perp} - \vec{k}_{1\perp}\right)^2 + \mu^2} \\
&= f\int \frac{d^2x_\perp}{(2\pi)^2} \left(\int \frac{d^2q_\perp}{q_\perp^2+\mu^2} e^{i\vec{x}_\perp \vec{q}_\perp}\right)^2 \int \frac{dk_{1\perp}}{k_{1\perp}} \int \frac{dk_{2\perp}}{k_{2\perp}} \\
&\quad \times \int d\phi_1 e^{i(\phi_1 n - x_\perp k_{1\perp}\cos(\phi_1))} e^{i\phi_x n} \int d\phi_2 e^{i(-\phi_2 n - x_\perp k_{2\perp}\cos(\phi_2))} e^{-i\phi_x n} \\
&= f\int \frac{d^2x_\perp}{(2\pi)^2} \left(2\pi K_0(\mu x_\perp)\right)^2 \int \frac{dk_{1\perp}}{k_{1\perp}} \\
&\quad \times \int \frac{dk_{2\perp}}{k_{2\perp}} \left[2\pi(-i)^n J_n(x_\perp k_{1\perp})\right] \left[2\pi(-i)^n J_n(x_\perp k_{2\perp}))\right] \\
&= \frac{(2\pi)^3 f}{2\mu^2} \frac{(-1)^n}{n^2} .
\end{aligned} \tag{3}$$

To derive this, we first applied Eq. (2) and then used the following well known integrals

$$\int \frac{d^2q_\perp}{q_\perp^2+\mu^2} e^{i\vec{x}_\perp \vec{q}_\perp} = 2\pi K_0(\mu x_\perp) , \tag{4}$$

$$\int d\phi_1 e^{i(\phi_1 n - x_\perp k_{1\perp}\cos(\phi_1))} = 2\pi(-i)^n J_n(x_\perp k_{1\perp}) , \tag{5}$$

where K and J are corresponding Bessel functions. For an integer n, $J_n(x) = (-1)^n J_{-n}(x)$. Eq. (3) is only true for $n > 0$. For $n = 0$, the integral $\int \frac{dk_\perp}{k_\perp} J_0(x_\perp k_\perp)$ is divergent and should be properly regularized at the saturation momentum μ

$$\begin{aligned}
\int\limits_{\mu}^{\infty} \frac{dk_\perp}{k_\perp} J_0(x_\perp k_\perp) &= \lim_{\varepsilon\to 0}\left(\int\limits_0^{\infty} k^\varepsilon \frac{dk_\perp}{k_\perp} J_0(x_\perp k_\perp) - \int\limits_0^{\mu} k^\varepsilon \frac{dk_\perp}{k_\perp} J_0(x_\perp k_\perp)\right) \\
&= \ln 2 - \gamma_E - \ln(\mu x_\perp)\,. \qquad (6)
\end{aligned}$$

We assumed that at a momentum below the saturation momentum, μ, other processes including multi-pomeron exchange would cut off the integration in Eq. (6) at the saturation momentum. If such cut-off would not occur, then one would need to replace μ with the natural QCD infrared cut-off Λ_{QCD}. This would bring logarithmic modification to Eq. (6), namely an additional term $\ln\frac{\mu}{\Lambda_{\mathrm{QCD}}}$. By carrying out an explicit computation, we checked that for any reasonable value of $Q_{\mathrm{s}}/\Lambda_{\mathrm{QCD}}$, the nature of the conclusions of this article does not change.

Using this result, we obtain for $n = 0$

$$\begin{aligned}
\frac{d^2\sigma_0}{dy_1 dy_2} &= f\int\frac{d^2k_{1\perp}}{k_{1\perp}^2}\int\frac{d^2k_{2\perp}}{k_{2\perp}^2}\int\frac{d^2q_\perp}{q_\perp^2+\mu^2}\frac{1}{\left(\vec{q}_\perp - \vec{k}_{1\perp} - \vec{k}_{1\perp}\right)^2 + \mu^2} \\
&= f\int d^2x_\perp\left(2\pi K_0(\mu x_\perp)\right)^2\left(\ln 2 - \gamma_E - \ln(\mu x_\perp)\right)^2 \\
&= (2\pi)^3 f\frac{1}{\mu^2}\,. \qquad (7)
\end{aligned}$$

Here and later, we will use the following integral

$$S_m = \int dx x (K_0(x))^2 (\ln(2) - \gamma_E - \ln(x))^m\,. \qquad (8)$$

The analytic expression for $S(m)$ is derived in Appendix A. Here, we note that $S_0 = 1/2$ and $S_2 = 1$. In this article, we use S_m only for even m motivated by the experiments which measure flow coefficients for even m; however the generalization of our results to odd m is straightforward.

Thus, for $\langle v_n^2\rangle$, we have

$$\left\langle v_n^2\right\rangle = \frac{\frac{d^2\sigma_n}{dy_1 dy_2}}{\frac{d^2\sigma_0}{dy_1 dy_2}} = \frac{(-1)^n}{2n^2}\,. \qquad (9)$$

The flow cumulants for two-particle correlation are defined according $v_n[2] = \sqrt{\langle v_n^2 \rangle}$. Thus, *e.g.* for $n = 2$, $v_n[2] = \frac{\sqrt{2}}{4}$. The factor of -1 for the odd $\langle v_n^2 \rangle$ is a consequence of the backward peaking of the two-particle correlation, and is distinctively different from hydrodynamical flow induced correlations.

We note that Eq. (9) is obtained for the integrated flow coefficients. The analytical results was obtained owing to the integration with respect to the momenta of the produced gluons, $k_{1\perp}$ and $k_{2\perp}$.

The two-particle correlation function $C_2(\Delta\phi)$ defined by

$$C_2(\Delta\phi) = \left(\frac{d^2\sigma_0}{dy_1 dy_2}\right)^{-1} \int \frac{d^2 k_{1\perp}}{k_{1\perp}^2} \int \frac{d^2 k_{2\perp}}{k_{2\perp}^2} \delta(\Delta\phi + \phi_1 - \phi_2) \frac{d^6\sigma}{dy_1 d^2 k_{\perp 1} dy_2 d^2 k_{\perp 2}} \tag{10}$$

can be analytically computed using

$$\delta(x) = \frac{1}{2\pi} \sum_{a=-\infty}^{\infty} e^{iax} \,. \tag{11}$$

Applying the same transformations as for $d^2\sigma_n / dy_1 dy_2$, we arrive to

$$C(\Delta\phi) = 1 + \frac{1}{2\pi} \sum_{a=1}^{\infty} \frac{(-1)^a}{a^2} \cos(a\Delta\phi) = 1 - \frac{\pi}{24} + \frac{1}{8\pi} \Delta\phi^2 \,. \tag{12}$$

This equation is correct for $|\Delta\phi| < \pi$.

4. $2m$-particle production

Analogously to Eq. (3)

$$\begin{aligned}
\frac{d^{2m}\sigma_n}{dy_1 dy_2 \dots dy_{2m}} &= f \int \frac{d^2 k_{1\perp}}{k_{1\perp}^2} e^{i\phi_1 n} \int \frac{d^2 k_{2\perp}}{k_{2\perp}^2} e^{i\phi_2 n} \dots \int \frac{d^2 k_{m\perp}}{k_{m\perp}^2} e^{i\phi_m n} \\
&\quad \times \int \frac{d^2 k_{m+1\perp}}{k_{m+1\perp}^2} e^{-i\phi_{m+1} n} \dots \int \frac{d^2 k_{2m\perp}}{k_{2m\perp}^2} e^{-i\phi_{2m} n} \\
&\quad \times \int \frac{d^2 q_\perp}{q_\perp^2 + \mu^2} \frac{1}{\left(\vec{q}_\perp - \sum_{i=1}^{m} \vec{k}_{i\perp}\right)^2 + \mu^2} \\
&= (-1)^{nm} \left(\frac{2\pi}{n}\right)^{2m} \frac{2\pi f}{2\mu^2}
\end{aligned} \tag{13}$$

for non-zero n. For $n=0$, we get

$$\begin{aligned}
\frac{d^{2m}\sigma_0}{dy_1 dy_2\dots dy_{2m}} &= f\int\frac{d^2k_{1\perp}}{k_{1\perp}^2}\int\frac{d^2k_{2\perp}}{k_{2\perp}^2}\dots\int\frac{d^2k_{m\perp}}{k_{m\perp}^2}\\
&\quad\times\int\frac{d^2k_{m+1\perp}}{k_{m+1\perp}^2}\dots\int\frac{d^2k_{2m\perp}}{k_{2m\perp}^2}\\
&\quad\times\int\frac{d^2q_\perp}{q_\perp^2+\mu^2}\frac{1}{\left(\vec{q}_\perp-\sum_{i=1}^m\vec{k}_{i\perp}\right)^2+\mu^2}\\
&= (2\pi)^{2m+1}\frac{fS_{2m}}{\mu^2}\,. \qquad (14)
\end{aligned}$$

Thus

$$\left\langle v_n^{2m}\right\rangle = \left(\frac{d^{2m}\sigma_0}{dy_1 dy_2\dots dy_{2m}}\right)^{-1}\frac{d^{2m}\sigma_n}{dy_1 dy_2\dots dy_{2m}} = \frac{1}{2S_{2m}}\frac{(-1)^{nm}}{n^{2m}}\,. \qquad (15)$$

The corresponding cumulants $v_n[2m]$ can be computed using expressions given in Appendix B. Here, we provide the numerical values:

$$\begin{aligned}
v_2[2] &= 0.353553\,, & (16)\\
v_2[4] &= 0.404931\,, & (17)\\
v_2[6] &= 0.40857\,, & (18)\\
v_2[8] &= 0.408991\,, & (19)\\
v_2[10] &= 0.409049\,, & (20)\\
v_2[12] &= 0.409057\,. & (21)
\end{aligned}$$

5. Inclusive production

Until this point, we consider *exclusive* production of gluons. In experiment, however, one measures m particles out of many $N \gg m$ created in a collision. The equations presented in the previous sections can be straightforwardly generalized to the case of the inclusive production. First, we consider two-particle production and then generalize it for m-particle production. To obtain the inclusive cross section, we need to integrate our gluons produced in three rapidity windows $y_{\min} < y' < y_1$, $y_1 < y' < y_2$ and $y_2 < y' < y_{\max}$. We assume that in each rapidity window, we produce i, j and l gluons correspondingly. One necessarily needs to some up i, j and k over all possible number of gluons. The momenta of the gluons we integrate out are denoted by $\vec{\kappa}_\perp$. Hence, the inclusive cross section for two-gluon production is given by

$$\frac{d^6\sigma^{\rm inc}}{d^2k_1dy_1d^2k_2dy_2} = \sum_{i=0}^{\infty}\sum_{j=0}^{\infty}\sum_{l=0}^{\infty}\frac{1}{i!}\frac{1}{j!}\frac{1}{l!}\frac{1}{(2\pi)^{2(i+j+k)}}$$
$$\times\prod_{i'=0}^{i+j+l}\int d^2\kappa_{i'\perp}d^2y'_{i'}\frac{d^{3(2+i+j+l)}\sigma}{d^2k_{1\perp}dy_1d^2k_{2\perp}dy_2d^2\kappa_{1\perp}dy'_1\dots d^2\kappa_{(i+j+l)\perp}dy'_{(i+j+k)}}$$
$$= f\int d^2x_\perp\int d^2q_\perp\frac{e^{i\vec{x}_\perp\vec{q}_\perp}}{q_\perp^2+\mu^2}\int\frac{d^2p_\perp}{(2\pi)^2}\frac{e^{i\vec{x}_\perp\vec{p}_\perp}}{p_\perp^2+\mu^2}\frac{e^{-i\vec{x}_\perp\vec{k}_{1\perp}}}{k_{1\perp}^2}\frac{e^{-i\vec{x}_\perp\vec{k}_{2\perp}}}{k_{2\perp}^2}$$
$$\times\sum_{i=0}^{\infty}\sum_{j=0}^{\infty}\sum_{l=0}^{\infty}\frac{1}{i!}\frac{1}{j!}\frac{1}{l!}\left(\frac{\alpha N_c}{\pi}\right)^{i+j+k}\prod_{i'=0}^{i+j+l}\int d^2\kappa_{i'\perp}d^2y'_{i'}\frac{e^{i\vec{x}_\perp\vec{\kappa}_{i'\perp}}}{\vec{\kappa}_{i'\perp}^2}$$
$$= f\int d^2x_\perp\left(\frac{2e^{-\gamma_E}}{\mu x_\perp}\right)^\beta K_0^2(\mu x_\perp)\frac{e^{-i\vec{x}_\perp\vec{k}_{1\perp}}}{k_{1\perp}^2}\frac{e^{-i\vec{x}_\perp\vec{k}_{2\perp}}}{k_{2\perp}^2}\,, \tag{22}$$

where $\beta=\frac{\alpha N_c}{\pi}\Delta y$ and $\Delta y=y_{\rm max}-y_{\rm min}$. Thus for $\langle v_n^2\rangle$, we have

$$\left\langle v_n^2\right\rangle=\frac{\tilde{S}_0}{\tilde{S}_2}\frac{(-1)^n}{n^2}\,. \tag{23}$$

Here,

$$\tilde{S}_m=\int dx x^{1-\beta}K_0^2(x)\left(\ln 2-\ln(x)-\gamma_E\right)^m \tag{24}$$

and can be computed by the help of the second part of Appendix A.

Similar and more tedious, but straightforward computations along the lines shown above result in

$$\left\langle v_n^{2m}\right\rangle=\frac{\tilde{S}_0}{\tilde{S}_{2m}}\frac{(-1)^{nm}}{n^{2m}}\,. \tag{25}$$

Using Appendix A and Appendix B, the flow coefficients can be computed for different values of β, here we provide the number for $\beta=1/2$

$$v_2[2] = 0.242046\,, \tag{26}$$
$$v_2[4] = 0.275329\,, \tag{27}$$
$$v_2[6] = 0.277706\,, \tag{28}$$
$$v_2[8] = 0.277986\,, \tag{29}$$
$$v_2[10] = 0.278025\,, \tag{30}$$
$$v_2[12] = 0.278031\,. \tag{31}$$

We want to point out that the selected value of β lies beyond the applicability of our model which is defined by $\alpha_{\rm s} N_c \Delta y \ll 1$; nonetheless our result vividly demonstrates that even for extreme values of β the higher order flow coefficients are equal to each other and the main conclusion of this article remain true. For smaller β, the absolute values of $v_2\{m\}$ will be closer to those listed in the previous section, where $\beta = 0$.

6. Summary and conclusions

We have shown that the flow analysis of the Pomeron indicates a pattern which certainly indicates collective motion of its decay products. We have been careful to restrict our consideration to processes where single Pomeron exchange is the dominant contribution. One might ask if it might be relevant for heavy-ion collisions. In the two-particle correlations of pA or pp collisions, the jet contribution is explicitly subtracted. If this is properly done, the Pomeron contribution should be removed, and the remainder is the diagram of Fig. 2. In addition, in pA or pp collisions, there are all possible manners of final state interactions which might generate collective effects.

In multi-particle correlations with numbers of particles greater than 2, no subtraction of the jet contributions done for pA collisions, so the Pomeron might make a significant contribution. However, it is important to remember that the collectivity of the Pomeron is really associated with a backwards recoil peak for the Pomeron as is shown in Fig. 3. This means that the computed $(v_n(4p+2))^{4p+2}$ would be negative for odd n. The first place this would appear would be in v_3 [6]. A measurement of such a correlation would give a solid measure of whether or not the collectivity in pA collisions arises from collectivity of Pomeron decays or other effects.

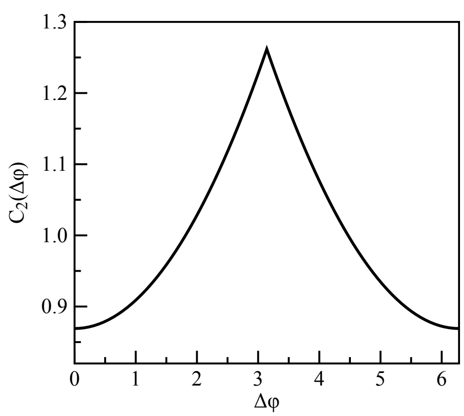

Fig. 3. $C_2(\Delta\phi)$ for two-particle production.

The collectivity seen in the Pomeron decay suggests that there will be entirely non-trivial patterns in other multi-particle processes. We would associate such collectivity with an initial state effect. Perhaps something along the lines of Ref. [14] or of Ref. [17] are steps in the correct direction for making a theory.

Even if there is little impact of these results for pA or pp collisions, the collectivity of the decay products observed for the Pomeron may have implications for elementary processes such as jet decay in e^+e^- annihilation of in deep inelastic scattering. A proper determination of such effects would require an analysis of the fragmentation of the gluons produced in such collisions.

We also note that the main result of this article $v_n[m] \approx v_n[p]$ holds for exclusive and inclusive gluon production.

The research of L.M. is supported under D.O.E. Contract No. DE-AC02-98CH10886. We thank Francois Gellis and Eugene Levin for very useful comments and discussions. Lary McLerran acknowledges very useful conversations with Miklos Gyulassy on this subject, and a most stimulating talk he gave at Quark Matter 2014, where these ideas were initiated.

Appendix A

$$S_m = \int dx x K_0^2(x) \left(\ln 2 - \ln(x) - \gamma_E\right)^m . \tag{32}$$

This integral can be taken analytically

$$S_m = \sum_{i=0}^{m} \binom{m}{i} \left(\ln 2 - \gamma_E\right)^{m-i} I_i \,, \tag{33}$$

where

$$I_i = (-1)^i \int dx x K_0^2(x) \ln^i(x) = (-1)^i \frac{d^i}{d\alpha^i} \left(\frac{\sqrt{\pi}}{4} \frac{\Gamma^3\left(\frac{\alpha+1}{2}\right)}{\Gamma(\alpha/2+1)} \right)\Bigg|_{\alpha=1} . \tag{34}$$

This integral can be derived from

$$\int K_0^2(x) x^\alpha dx = \frac{\sqrt{\pi}}{4} \frac{\Gamma^3\left(\frac{\alpha+1}{2}\right)}{\Gamma(\alpha/2+1)} \,. \tag{35}$$

Some values for S_m are

$$S_0 = 1/2\,, \tag{36}$$
$$S_1 = 1/2\,, \tag{37}$$
$$S_2 = 1\,, \tag{38}$$
$$S_4 = -2\zeta(3) + 12 - \frac{\pi^4}{40}\,, \tag{39}$$
$$S_6 = -60\zeta(3) + 5\zeta(3)^2 - 63\zeta(5) + 360 - \frac{3\pi^4}{4} - \frac{5\pi^6}{84}\,. \tag{40}$$

All factors of $\ln 2$ appearing on the right-hand side of Eq. (32) cancel in the final expressions for S_m.

Similarly, for the inclusive cross section, we compute

$$\tilde{S}_m = \int dx x^{1-\beta} K_0^2(x) \left(\ln 2 - \ln(x) - \gamma_E\right)^m = \sum_{i=0}^{m} \binom{m}{i} (\ln 2 - \gamma_E)^{m-i} \tilde{I}_i\,, \tag{41}$$

where

$$\tilde{I}_i = (-1)^i \int dx x^{1+\beta} K_0^2(x) \ln^i(x) = (-1)^i \frac{d^i}{d\alpha^i} \left(\frac{\sqrt{\pi}}{4} \frac{\Gamma^3\left(\frac{\alpha+1}{2}\right)}{\Gamma(\alpha/2+1)} \right)\Bigg|_{\alpha=1-\beta}\,. \tag{42}$$

Appendix B

For completeness, here we also list the expressions for the cumulants

$$v_n[2]^2 = \left\langle v_n^2 \right\rangle\,, \tag{43}$$
$$v_n[4]^4 = 2\left\langle v_n^2 \right\rangle^2 - \left\langle v_n^4 \right\rangle\,, \tag{44}$$
$$v_n[6]^6 = \tfrac{1}{4}\left(12\left\langle v_n^2 \right\rangle^3 - 9\left\langle v_n^4 \right\rangle\left\langle v_n^2 \right\rangle + \left\langle v_n^6 \right\rangle \right)\,, \tag{45}$$
$$\begin{aligned} v_n[8]^8 = \tfrac{1}{33}\Big(& 144\left\langle v_n^2 \right\rangle^4 - 144\left\langle v_n^4 \right\rangle\left\langle v_n^2 \right\rangle^2 + 16\left\langle v_n^6 \right\rangle\left\langle v_n^2 \right\rangle \\ & +18\left\langle v_n^4 \right\rangle^2 - \left\langle v_n^8 \right\rangle \Big)\,, \end{aligned} \tag{46}$$
$$\begin{aligned} v_n[10]^{10} = \tfrac{1}{456}\Big(& 2880\left\langle v_n^2 \right\rangle^5 - 3600\left\langle v_n^4 \right\rangle\left\langle v_n^2 \right\rangle^3 + 400\left\langle v_n^6 \right\rangle\left\langle v_n^2 \right\rangle^2 \\ & + 25\left(36\left\langle v_n^4 \right\rangle^2 - \left\langle v_n^8 \right\rangle \right)\left\langle v_n^2 \right\rangle - 100\left\langle v_n^4 \right\rangle\left\langle v_n^6 \right\rangle + \left\langle v_n^{10} \right\rangle \Big)\,. \end{aligned} \tag{47}$$

REFERENCES

[1] I.I. Balitsky, L.N. Lipatov, *Sov. J. Nucl. Phys.* **28**, 822 (1978) [*Yad. Fiz.* **28**, 1597 (1978)].

[2] L.V. Gribov, E.M. Levin, M.G. Ryskin, *Phys. Rep.* **100**, 1 (1983).

[3] A.H. Mueller, J.-w. Qiu, *Nucl. Phys. B* **268**, 427 (1986).

[4] L.D. McLerran, R. Venugopalan, *Phys. Rev. D* **49**, 2233 (1994) [`arXiv:hep-ph/9309289`].

[5] L.D. McLerran, R. Venugopalan, *Phys. Rev. D* **49**, 3352 (1994) [`arXiv:hep-ph/9311205`].

[6] B. Alver, G. Roland, *Phys. Rev. C* **81**, 054905 (2010) [*Erratum ibid.* **82**, 039903 (2010)] [`arXiv:1003.0194 [nucl-th]`].

[7] J. Adams *et al.* [STAR Collaboration], *Phys. Rev. C* **72**, 014904 (2005) [`arXiv:nucl-ex/0409033`].

[8] V. Khachatryan *et al.* [CMS Collaboration], *J. High Energy Phys.* **1009**, 091 (2010) [`arXiv:1009.4122 [hep-ex]`].

[9] S. Chatrchyan *et al.* [CMS Collaboration], *Phys. Lett. B* **718**, 795 (2013) [`arXiv:1210.5482 [nucl-ex]`].

[10] P. Bozek, W. Broniowski, *Phys. Lett. B* **718**, 1557 (2013) [`arXiv:1211.0845 [nucl-th]`].

[11] A. Dumitru, F. Gelis, L. McLerran, R. Venugopalan, *Nucl. Phys. A* **810**, 91 (2008) [`arXiv:0804.3858 [hep-ph]`].

[12] A. Dumitru *et al.*, *Phys. Lett. B* **697**, 21 (2011) [`arXiv:1009.5295 [hep-ph]`].

[13] K. Dusling, R. Venugopalan, *Phys. Rev. Lett.* **108**, 262001 (2012) [`arXiv:1201.2658 [hep-ph]`].

[14] M. Gyulassy, P. Levai, I. Vitev, T. Biro, *Phys. Rev. D* **90**, 054025 (2014) [`arXiv:1405.7825 [hep-ph]`].

[15] J.F. Gunion, G. Bertsch, *Phys. Rev. D* **25**, 746 (1982).

[16] D. Kharzeev, E. Levin, L. McLerran, *Nucl. Phys. A* **748**, 627 (2005) [`arXiv:hep-ph/0403271`].

[17] A. Dumitru, A.V. Giannini, *Nucl. Phys. A* **933**, 212 (2015) [`arXiv:1406.5781 [hep-ph]`].